

## Cordierites: compositional controls of $\Delta$ , cell parameters, and optical properties

KEVIN R. SELKREGG<sup>1</sup> AND F. DONALD BLOSS

Department of Geological Sciences  
Virginia Polytechnic Institute and State University  
Blacksburg, Virginia 24061

### Abstract

For natural cordierites (except for indialites), the cell-edge variations which cause variations in the distortion index  $\Delta$  more likely represent differences in composition than in Al/Si ordering. Back-reflection Weissenberg data from 11 cordierite grains representing atomic ratios  $(\text{Fe} + \text{Mn})/(\text{Fe} + \text{Mn} + \text{Mg})$  from 0.046 to 0.898 reveal that, with increase in  $R_a$  (the average radius of the ions occupying the octahedral sites), cell edges  $a$  and  $b$  increase linearly whereas  $c$  decreases until  $R_a$  exceeds *ca.* 0.765, then apparently increases. Statistical analyses on data for unheated grains reveal  $\Delta$  to decrease markedly as  $x$  (mole fraction Na) increases, increase moderately as  $R_a$  increases, but seem relatively independent of  $\text{H}_2\text{O}$ , probably because the strong correlation between Na and  $\text{H}_2\text{O}$  content in unheated cordierites partially masked the effect of  $\text{H}_2\text{O}$  on  $\Delta$ . In contrast,  $\Delta$  increased significantly when four cordierites were heated at  $800^\circ\text{C}$  with  $\text{H}_2\text{O}$  being driven off. Inclusion of these data in the regression analysis revealed  $\text{H}_2\text{O}$  content, as suggested by Stout (1975), to have a significant effect on  $\Delta$ . For a natural Na,Be cordierite, Schreyer (1979) confirmed this by changing its  $\Delta$  value from  $0.12^\circ$  to  $0.26^\circ$  by dehydration, then returning it to  $0.11^\circ$  by rehydration.

The optical data, remeasured for 10 grains after their partial dehydration at  $800^\circ\text{C}$  for six hours in a slowly flushing  $\text{H}_2$  atmosphere, showed reduction of all refractive indices and yielded remarkably regular curves relating the indices  $\alpha$ ,  $\beta$ , and  $\gamma$  to  $(\text{Fe} + \text{Mn})/(\text{Fe} + \text{Mn} + \text{Mg})$  ratio. Exceptions were two specimens high in Na and Be whose indices, even after heating, exceed the general trends. As for  $\Delta$ , heating increased  $2V_x$  ( $\lambda = 666 \text{ nm}$ ) except for the two optically (+) grains which show slight decreases. Prior to heating,  $2V_x$  correlates inversely with  $\text{H}_2\text{O}$  whereas, after partial dehydration at  $800^\circ\text{C}$ ,  $2V_x$  correlates inversely with Na content and, less certainly, with  $R_a$ .

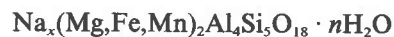
### Introduction

Miyashiro (1957) introduced the distortion index

$$\Delta = 2\theta_{131} - (2\theta_{511} + 2\theta_{421})/2 \quad (1)$$

to monitor, with  $\text{CuK}\alpha_1$  peaks, the deviation of cordierite's C-centered orthorhombic lattice (indexed  $c < b < a$ ) from hexagonal geometry. He then presumed natural cordierites to represent a continuous order-disorder series ranging from complete Al/Si ordering in the  $\text{Si}_5\text{AlO}_{18}$  rings (orthorhombic,  $\Delta \approx 0.30^\circ$ ) to complete disordering ( $\Delta \approx 0^\circ$ ). Gibbs (1966) established cordierite as a framework structure and suggested that any Al/Si order-disorder transformation would involve this entire framework.

The  $\text{Al}_4\text{Si}_5\text{O}_{18}$  framework of cordierite consists of superimposed  $\text{Al}_2\text{Si}_4\text{O}_{18}$  rings linked laterally and vertically by 2Al and 1Si in tetrahedral coordination. This superposition of rings forms channels parallel to  $c$ . These consist of large spheroidal cavities (radius  $\approx 2.2\text{\AA}$ ) connected by smaller "bottle neck" openings (radius  $\approx 1.4\text{\AA}$ ), which are actually the central openings of the individual rings. The channel occupants are principally  $\text{H}_2\text{O}$  but also  $\text{Na}^+$ ,  $\text{Ca}^{2+}$ —or, less frequently,  $\text{Fe}^{2+}$ ,  $\text{K}^+$ ,  $\text{Li}^+$ ,  $\text{Rb}^+$ , or  $\text{Cs}^+$ . The octahedral sites within the framework accommodate  $\text{Mg}^{2+}$ ,  $\text{Fe}^{2+}$ , and, to a lesser extent,  $\text{Mn}^{2+}$ . A formula that includes the more frequent of the channel occupants is thus



Important compositional variables will thus be:  $x$ , the Na ions per formula unit;  $F$ , the mole fraction  $(\text{Fe} + \text{Mn})/(\text{Fe} + \text{Mn} + \text{Mg})$  that describes occupancy of

<sup>1</sup> Present address: The Carborundum Company, Advanced Technology Branch, Refractories Division, P. O. Box 367, Niagara Falls, New York 14302.

the octahedral sites; and  $n$ , which usually takes values up to 1.0 ( $\approx$  3 weight percent H<sub>2</sub>O or one H<sub>2</sub>O molecule per spheroidal cavity). However, the custom of expressing H<sub>2</sub>O contents of cordierites in weight percent has led us to use, in subsequent equations, the symbol H<sub>2</sub>O to represent weight percent water. Analyses of natural cordierites (Leake, 1960; Lepezin *et al.*, 1976) reveal that H<sub>2</sub>O rarely exceeds 3 weight percent.

The reliability of  $\Delta$  as a measure of Al/Si ordering has been questioned by Gibbs (1966) and Meagher (1967), largely because it seemed sensitive to chemical variations. Furthermore, Povondra and Langer (1971) observed  $\Delta$  in synthetic cordierites to decrease with increased Na<sup>+</sup> and Be<sup>2+</sup> content, Be<sup>2+</sup> evidently replacing tetrahedral Al<sup>3+</sup> with Na<sup>+</sup> concomitantly occupying channel sites. Stout (1975) concluded that the  $\Delta$  index increased with Al/Si ordering but decreased with H<sub>2</sub>O content. This met an objection by Langer and Schreyer (1976), who concluded that the relatively low  $\Delta$  value of the Haddam cordierite could be "explained on the basis of its Na + Be content alone, and water may be without significance." Kamineni (1974) observed  $\Delta$  to increase with substitution of Fe<sup>2+</sup> for Mg<sup>2+</sup> in the octahedral sites but, influenced by the study of Harwood and Larson (1969), attributed the correlation to "thermal history."

To our knowledge, no publication has stated that (1) variations in  $\Delta$  are primarily compositional in origin for natural orthorhombic cordierites, and (2) significant Al/Si disordering exists only for the extreme case of indialites. Establishing these two points should remove some barriers to our understanding of the crystal optics and crystal chemistry of natural cordierites. Until now, the anomalies so apparent in plots of  $2V_x$  vs.  $F$  have been linked with Al/Si ordering (because  $2V_x$  correlates so strongly with  $\Delta$  that it is frequently suggested as an alternate measure of Al/Si ordering). Similarly, when Iiyama (1956) greatly reduced the scatter in plots of refractive indices against  $F$  by first heating the grains at 1000°C for 10 minutes, he believed he had standardized their structural state. Later, after Schreyer and Yoder (1964) demonstrated the mean refractive index for synthetic Mg-cordierites to increase with H<sub>2</sub>O content, it became apparent that Iiyama's heat treatment had merely dehydrated the cordierites and thereby reduced the diversity in their H<sub>2</sub>O contents (and indices).

The positive relationship between refractive index and H<sub>2</sub>O content of cordierites has been amply dem-

onstrated by Lepezin *et al.* (1976), who present equations whereby H<sub>2</sub>O content can be calculated provided  $F$  and either  $\alpha_D$  or  $\gamma_D$  are known.<sup>2</sup> Our multiple linear regressions performed on their data for 21 cordierites indicate that the null hypothesis (that H<sub>2</sub>O content has no effect on the refractive index  $\alpha$  or  $\gamma$ ) can be rejected only at a significance level of 0.0001. The positive effect of H<sub>2</sub>O content on  $\alpha$  and  $\gamma$  thus seems established beyond reasonable doubt.

This study was initiated to clarify and quantify the relationships between optical properties, lattice geometry,  $\Delta$ , and crystal chemistry for the cordierite series. The time seemed ripe since spindle stage techniques permit: (1) precise measurement of a grain's refractive indices and  $2V$ ; (2) transfer of this grain to a back-reflection Weissenberg camera for precise measurement of its cell edges; and, ultimately, (3) microprobe analyses of this grain.

## Experimental methods

### Optical

Single crystals of cordierite were mounted on goniometer heads which were then attached to a Supper spindle stage. The stage positions that caused extinction between crossed nicols were determined photometrically (*cf.* Bloss, 1978) for wavelengths 400, 666, and 900 nm as the spindle stage was successively set at 0°, 10°, 20° . . . 350°. The resultant data, submitted to EXCALIBUR, the Bloss and Riess (1973) program as revised by Michael Rohrer and Bloss, yielded values for  $2V_{400}$ ,  $2V_{666}$ , and  $2V_{900}$ . Also calculated were the setting of the spindle stage ( $S$ ) and microscope stage ( $M_s$ ) which orient the grain so that principal indices  $\alpha$ , then  $\beta$ , then  $\gamma$  can be measured from it without appreciable error from crystal misorientations. Each principal index was measured by the double-variation method using an oil cell, with heating element and thermocouple, specially built for the Supper spindle stage. Following Louisnathan *et al.* (1978), two constants  $a_0$  and  $a_1$  were determined for each principal index. These, inserted into the linearized Sellmeier equation

$$y = a_0 + a_1x$$

where  $y$  represents  $(n^2 - 1)^{-1}$  and  $x$  represents  $\lambda^{-2}$ , permit the principal index to be calculated for any desired wavelength. The method, applied to optical

<sup>2</sup> Lepezin *et al.* (1976) transpose  $\alpha$  and  $\gamma$  throughout their paper and use  $F$  to represent *mole percent* whereas here we use  $F$  to denote *mole fraction* of Fe plus Mn in the octahedral sites.

glasses whose absolute indices were known to the fifth decimal, reproduced  $n_D$  to within 0.0005. Indices calculated for wavelengths beyond the visible were less accurate because the equation is only linear over a limited wavelength range (and was fitted to indices for visible wavelengths).

While determining the crystal extinction positions at wavelengths 400, 666, and 900 nm, the crystal was immersed in an oil whose index matched the  $\beta$  index of the grain for that wavelength. This precaution, together with determining the extinction data for a full 360° rotation of the spindle stage (instead of just 180°), reduced errors in extinction measurements—and thus in  $2V$ —caused by refraction of the light at grain–oil interfaces oblique to the light beam.

### X-ray

From the optical extinction data, EXCALIBUR calculated the spindle-stage coordinates ( $S$ ,  $E$ ) for the principal vibration axes  $X$ ,  $Y$ , and  $Z$  for each cordierite grain. From these coordinates, since cordierite is orthorhombic, one can calculate the changes in the goniometer arc settings necessary to align a direct crystallographic axis parallel to the dial axis of the X-ray camera to which the goniometer head is transferred; Bloss (in press) describes these simple equations and techniques in detail. Lattice parameters of the specimens were determined with a precision back-reflection Weissenberg camera and unfiltered Cu-radiation. The  $2\theta$  values for the indexed  $\text{CuK}\alpha_1$ ,  $\text{CuK}\alpha_2$ ,  $\text{CuK}\beta$  reflections were submitted to the least-squares refinement program of Burnham (1962, 1965), revised by L. Finger, which corrects for systematic errors from film shrinkage, absorption, and eccentricity. Between 45 and 70 reflections were indexed for each specimen.

### Heating

After the preceding optical and X-ray measurements on the 11 cordierite grains selected for study, 10 were removed from their glass fibers, placed in silver capsules, and heated in a flushing  $\text{H}_2$  atmosphere for six hours at 800°C in a Lindberg Hevi-duty electric furnace (Type 55031-A). After heating, the optical properties were remeasured for the 10 grains, and the cell edges for only four. In preliminary heating experiments the iron-rich Dolni Bory grains, when heated in air or even in a flushing inert-gas atmosphere ( $\text{N}_2$ ), developed a rust-colored coating, presumably hematite, that prevented further optical study. Heating in a flushing  $\text{H}_2$  atmosphere largely overcame the problem, although even so the Dolni

Bory grain studied optically did develop some amorphous almost submicroscopic spherical inclusions after heating. These constituted less than 1% by volume of the grain, showing a tendency to be concentrated at the grain's surface and along fractures. Fortunately, amorphous inclusions do not deter the photometric measurement of crystal extinction.

The temperature and duration of heating adopted were arrived at, in part, empirically. Goldman *et al.* (1977) reported that at 800°C cordierite lost all its  $\text{H}_2\text{O}$ . Duration of heating was decided upon after heating a grain of the Dolni Bory cordierite at 800°C in a flushing  $\text{H}_2$  atmosphere for 1, 3, 6, and 8 hours, then determining  $2V_x$  after each run. After about six hours heating time,  $2V_x$  stabilized in value.

## Results and observations

### Specimens and primary data

Table 1 identifies the 11 natural cordierites studied, assigns reference numbers from 1 to 11, and presents results of the microprobe analyses that concluded their study. These microprobe analyses permitted calculation of  $F$  (previously defined) and of  $R_a$ , the average radius of the ions presumed to fill the octahedral sites. Thus

$$R_a = 0.72x_{\text{mg}} + 0.78x_{\text{fe}} + 0.83x_{\text{mn}}$$

where  $x_{\text{mg}}$ ,  $x_{\text{fe}}$  and  $x_{\text{mn}}$  respectively represent the mole fractions of  $\text{Mg}^{2+}$ ,  $\text{Fe}^{2+}$ ,  $\text{Mn}^{2+}$  in the octahedral sites and 0.72, 0.78, and 0.83 are Shannon's (1976) radii for these ions if six-coordinated.

Table 2 summarizes the optical parameters measured for the crystals before and, except for #3, after heating. Table 3 summarizes the unit-cell data for these crystals before heating and—for #1, #2, #6 and #11—after heating. From the cell edges,  $2\theta_{131}$ ,  $2\theta_{511}$ , and  $2\theta_{421}$  were calculated for  $\text{CuK}\alpha_1$ , so as to determine  $\Delta$ . An overwhelming correlation exists between  $\Delta$  and the difference  $(a - b\sqrt{3})$ . The linear equation relating them ( $r^2 = 0.999$ )

$$\Delta = 1.094 (a - b\sqrt{3})$$

provides a quick means of calculating  $\Delta$  (to within ca. 0.003°).

### Compositional changes from heating

Previous workers heated cordierites in air (Iiyama, 1956; Miyashiro, 1957) and, in consequence, oxidation of  $\text{Fe}^{2+}$  occurred. Although Hochella *et al.* (1979) heated the White Well cordierite *in vacuo*, oxi-

Table 1. Compositions\* of cordierites and locality descriptions

Specimen	Na	Mg	Mn	Fe**	$\frac{\text{Fe}+\text{Mn}}{\text{Fe}+\text{Mn}+\text{Mg}}$	$R_a$	Locality
(1) White Well	0.05	1.88	0.0	0.09	0.046	0.723	Sill-drav-cord-phlog schist body. White Well, Western Australia. (Pryce, 1973)
(2) Casper	0.04	1.76	0.0	0.23	0.114	0.727	Ann Trevett mine. Casper, Wyoming.
(3) SN72229	0.02	1.67	0.02	0.32	0.159	0.730	Opx-alm-cord-biot-Ksp metapelite. Snyder Bay, Labrador. (Speer, 1976)
(4) Guilford	0.07	1.55	0.02	0.45	0.233	0.734	Peg-qtz-plag vein. Guilford, Connecticut. (Schreyer, 1959)
(5) Pielosca	0.03	1.46	0.01	0.55	0.277	0.737	Pielosca, Finland.
(6) Haddam***	0.27	1.34	0.02	0.58	0.310	0.739	Pegmatite cutting biotite gneiss. Haddam, Connecticut. (Miyashiro, 1957)
(7) Ghost Lake	0.03	1.21	0.0	0.77	0.389	0.743	Bio-gar-cord-sill-hyp metasediment. Ghost Lake, NWT, Canada. (Robertson and Folinsbee, 1974)
(8) SN72123	0.02	0.86	0.0	1.12	0.567	0.754	Plag-cord-qtz-sill-Ksp quartzite. Snyder Bay, Labrador. (Speer, 1976)
(9) Sugama***	0.33	0.49	0.20	1.17	0.745	0.770	Granitic pegmatite cutting gneissic hbl-bio granodiorite. Sugama, Hukusima Prefecture, Japan. (Miyashiro, 1957)
(10) SN72189	0.03	0.53	0.0	1.43	0.727	0.764	Ksp-qtz-sill-plag-cord quartzite. Snyder Bay, Labrador (Speer, 1976)
(11) Dolni Bory	0.20	0.19	0.08	1.61	0.898	0.776	Pegmatite. Dolni Bory, W. Moravia, Czechoslovakia. (Stanek and Miskovsky, 1964)

\*Values listed in formula units. K, Ca, and Ti were observed to be less than 0.01 atoms in all cases.

\*\*Fe assumed FeO.

\*\*\*Formula units calculated on the basis of five silicons. This resulted in 3.76 Al in the Haddam and 3.77 Al in the Sugama. All others have Al and Si in 4:5 ratio. On the basis of Be/Si ion yield ratios, the Sugama contains about twice as much Be<sup>2+</sup> as the Haddam which contains 0.5 weight percent BeO (Newton, 1966).

dation still occurred, powder rings for secondary hematite appearing in precession photographs of the heated sample. By contrast, precession photographs of the heated White Well specimen in this study showed no powder rings.

The most common compositional change after heating is loss of molecular H<sub>2</sub>O from the channels.

Schreyer and Yoder (1964) observed rapid and complete dehydration to occur above 750°C for powdered Mg-cordierite (~1-micron grains). Goldman *et al.* (1977) report complete dehydration of a 0.5-mm-thick slab cut parallel to (100), but no appreciable loss of Na or Fe, after 2 hours at 800°C. For the White Well cordierite at 775°C in an evacuated cap-

Table 2. Optical parameters for cordierite grains before heating (upper line) and after heating (lower line)

Refractive Indices (589.3 nm)			2V <sub>x</sub> (EXCALIBR)			
α	β	γ	2V*	400	666	900
#1 White Well						
1.5345	1.5392	1.5423	77.9	75.81	76.41	77.04
1.5234	1.5260	1.5282	85.1	86.65	87.73	88.22
#2 Casper						
1.5313	1.5355	1.5399	91.1	92.23	91.02	91.05
1.5257	1.5290	1.5320	87.1	89.20	89.76	89.90
#3 SN72229**						
1.5316	1.5355	1.5389	85.9	85.54	81.74	85.32
#4 Guilford						
1.5396	1.5452	1.5485	74.8	74.16	73.38	73.64
1.5286	1.5324	1.5361	89.0	83.86	84.33	84.24
#5 Pielosca						
1.5358	1.5408	1.5461	91.4	92.27	89.26	84.64
1.5301	1.5343	1.5379	85.4	87.82	86.32	87.55
#6 Haddam						
1.5501	1.5580	1.5593	44.0	43.85	43.46	42.57
1.5337	1.5395	1.5419	65.3	71.89	69.99	69.45
#7 Ghost Lake						
1.5407	1.5470	1.5516	80.1	84.69	84.5	84.31
1.5335	1.5382†	1.5425	86.6	85.85	86.57	87.05
#8 SN72123						
1.5449	1.5522	1.5581	83.5	85.33	80.83	80.93
1.5384	1.5444†	1.5496	85.4	86.98	85.41	84.73
#9 Sugama						
1.5610	1.5726	1.5754	52.0	55.29	55.22	55.30
1.5510	1.5573	1.5589	53.3	-	69.34	70.85
#10 SN72189						
1.5491	1.5572	1.5636	82.9	84.87	81.53	81.18
1.5426	1.5499	1.5561	84.8	87.61	84.22	82.31
#11 Dolni Bory						
1.5601	1.5709	1.5761	69.1	67.86	63.17	63.33
1.5476	1.5565	1.5626	78.8	77.0	75.13	72.80

\*Calculated from indices.

\*\*Only unheated results.

†2V<sub>666</sub> used to calculate β refractive index.

sule, Hochella *et al.* (1979) observed no O<sub>w</sub> peak—namely, the oxygen peak associated with the H<sub>2</sub>O molecule—whereas the peak associated with the alkali ions persisted, albeit enlarged. After the sample was cooled to 24°C, the O<sub>w</sub> peak reappeared but at less than half its original intensity. Possibly the partial pressure of H<sub>2</sub>O had built up in the capsule during heating and H<sub>2</sub>O reentered the channels upon cooling the sample to 24°C.

To determine if the heat treatment had altered composition (other than by dehydration), grains of the Haddam, Casper, Ghost Lake, Sugama, and Dolni Bory cordierites were fragmented and some of these fragments were subjected to the same heat

treatment as those studied optically. Comparison of the microprobe analyses for these heated and unheated fragments indicated no appreciable loss of Na or any other cations with heating.

### Refractive indices and F value

A plot of principal refractive indices vs. *F* (Fig. 1) shows regular trends only after heating. Linear regressions of refractive indices on *F*, performed on the data for the heated low-Na (*x* < 0.08) cordierites (all but specimens 6, 9, and 11), yielded the following equations, *r*<sup>2</sup> at 0.999, with standard error of estimate for each parameter in parentheses below it:

$$\alpha = 1.5223 + 0.0282F \quad (2)$$

(0.0002) (0.0002) (0.0004)

$$\beta = 1.5246 + 0.0348F \quad (3)$$

(0.0003) (0.0002) (0.0004)

Table 3. Cell parameters\* for cordierite grains before heating and, if in italics, after heating

a	b	c	V	Δ**
(1) White Well cordierite				
17.065(3)	9.724(1)	9.346(1)	1550.9(5)	0.245
<i>17.079(2)</i>	<i>9.718(1)</i>	<i>9.344(1)</i>	<i>1550.8(5)</i>	<i>0.274</i>
(2) Casper cordierite				
17.074(3)	9.724(2)	9.341(1)	1550.8(6)	0.256
<i>17.094(1)</i>	<i>9.723(1)</i>	<i>9.340(1)</i>	<i>1552.4(2)</i>	<i>0.280</i>
(3) Cordierite SN 72229				
17.096(1)	9.727(1)	9.336(1)	1552.4(3)	0.274
(4) Guilford cordierite				
17.095(2)	9.742(1)	9.336(1)	1554.8(3)	0.243
(5) Pielosca cordierite				
17.115(1)	9.742(1)	9.327(1)	1555.2(2)	0.265
(6) Haddam cordierite				
17.050(1)	9.762(1)	9.326(1)	1552.2(2)	0.157
<i>17.072(2)</i>	<i>9.754(1)</i>	<i>9.329(1)</i>	<i>1553.4(3)</i>	<i>0.196</i>
(7) Ghost Lake cordierite				
17.140(3)	9.753(1)	9.319(1)	1557.8(5)	0.271
(8) Cordierite SN 72123				
17.180(1)	9.771(1)	9.308(1)	1562.4(2)	0.281
(9) Sugama cordierite				
17.133(2)	9.813(1)	9.302(1)	1563.9(3)	0.148
(10) Cordierite SN 72189				
17.223(2)	9.786(1)	9.309(1)	1567.2(4)	0.297
(11) Dolni Bory cordierite				
17.208(1)	9.830(1)	9.304(1)	1573.7(2)	0.198
<i>17.233(1)</i>	<i>9.818(1)</i>	<i>9.305(1)</i>	<i>1574.4(3)</i>	<i>0.247</i>

\*Standard errors in parentheses refer to the last digit.

\*\*Calculated (in degrees) from cell edges for CuKα<sub>1</sub>.

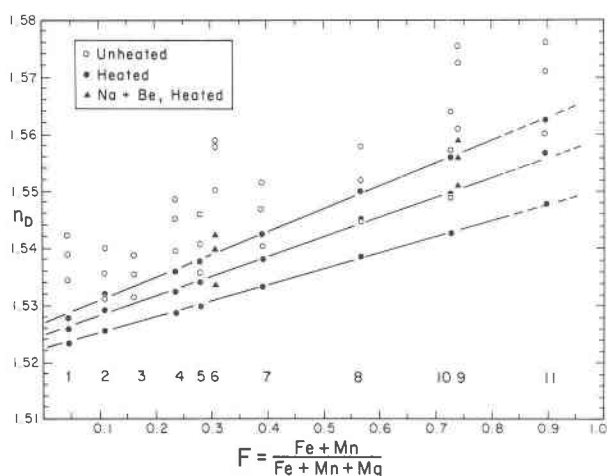


Fig. 1. Refractive indices  $\alpha$ ,  $\beta$ , and  $\gamma$  vs. atomic ratio  $F$  for unheated cordierite grains #1 to #11 (open circles) and for these same grains after heating at 800°C for six hours (filled circles or triangles).

$$\gamma = 1.5268 + 0.0403F \quad (4)$$

(0.0003) (0.0002) (0.0006)

Eq. 2 and 4 compare with those obtained by Lepezin *et al.* (1976) from data for 21 cordierites annealed at 1100°C in a vacuum ( $10^{-4}$  to  $10^{-5}$  torr) for 30 hours:

$$x = 1.5212 + 0.029F \quad (5)$$

$$\gamma = 1.5270 + 0.037F \quad (6)$$

Of the high-Na specimens (#6,  $x = 0.27$ ; #9,  $x = 0.33$ ; #11,  $x = 0.20$ ), only #11 lacked detectable BeO. For another specimen of #6, Newton (1966) reported 0.5 weight percent BeO; and an ion probe analysis of #9 indicated almost double that amount. After heating, the indices for #11 plotted on the regression line (Fig. 1) but those for #6 and #9 plotted above, roughly in proportion to their Be content. The higher post-heating indices for #6 and #9 likely stem from retention of H<sub>2</sub>O rather than from the direct effect of Be (plus channel Na) substituting for Al. In support, a Gladstone–Dale calculation indicated that even if Be substituted into one-tenth of the Al sites (hence,  $x = 0.40$ ), a cordierite's mean refractive index would increase by only 0.001. Moreover, Povondra and Langer (1971) observed refractive index to increase only slightly as Na,Be content increased in dry synthetic cordierites whereas, for comparable cordierites synthesized hydrothermally, the mean index exceeded that for the dry cordierites by 0.010. Thus incomplete dehydration after heating likely causes the higher post-heating indices of #6 and #9. Possibly the combination of high Na plus Be—or the presence of Na above a threshold of  $x = 0.20$  (or higher)—

permits Na to seal the water into the channels. Thus Černý and Hawthorne (1976) reported easier dehydration, with heating, for alkali-poor and Cs-free cordierites. They cited, for the isostructural mineral beryl, investigations wherein dehydration at high temperatures was impeded by high alkali content. More recently for beryl, Hawthorne and Černý (1977) concluded that Na is bonded to at least one, and possibly two, H<sub>2</sub>O molecule(s) in the channel.

For cordierites heated at 800°C as described,  $F$  may be estimated from the following equations obtained by linear regression ( $r^2 = 0.999$ ) on our data for low-Na ( $x < 0.08$ ) Be-free cordierites:

$$F = -53.914 + 35.417\alpha \quad (7)$$

(0.008) (0.719) (0.469)

$$F = -43.743 + 28.691\beta \quad (8)$$

(0.007) (0.547) (0.356)

$$F = -37.846 + 24.788\gamma \quad (9)$$

(0.009) (0.544) (0.353)

For the Dolni Bory specimen (#11), whose data were not used in the regression because of its high Na content ( $x = 0.20$ ), its microprobe-determined  $F$  value of 0.898 compares closely with  $F$  values estimated from its post-heating refractive indices, namely: 0.897 (from Eq. 7), 0.915 (Eq. 8), and 0.888 (Eq. 9). Eq. 7 to 9 may thus apply to cordierites with  $x$  as high as 0.20 provided they are Be-free. For Be-rich specimens the equations yield  $F$  values that are erroneously high, roughly in proportion to the Be content.

#### Estimated H<sub>2</sub>O contents

In the absence of analyses for H<sub>2</sub>O of the 11 grains examined, weight percent H<sub>2</sub>O was estimated (*esd* 0.13 weight percent) from the equations of Lepezin *et al.* (1976)

$$\text{H}_2\text{O} = 132.979 (\alpha + \gamma)/2 - 4.4F - 202.667 \quad (10)$$

and of Medenbach *et al.* (1979)

$$\text{H}_2\text{O} = [(\alpha + \gamma) - (\alpha_{\text{Dry}} + \gamma_{\text{Dry}})]/0.01524 \quad (11)$$

where  $\alpha_{\text{Dry}}$  and  $\gamma_{\text{Dry}}$  represent the grain's refractive indices after heating has completely dehydrated it. Our multiple linear regression analysis<sup>3</sup> of the data of Lepezin *et al.* (1976, their Tables 2 and 5) yielded two models

<sup>3</sup> The SAS stepwise procedure (Barr *et al.*, 1976) with all five options (forward selection, backward elimination, stepwise, maximum R<sup>2</sup> improvement, and minimum R<sup>2</sup> improvement) was used throughout this study.

$$\text{H}_2\text{O} = 141.337\alpha - 4.018F - 215.039 \quad (12)$$

$$\text{H}_2\text{O} = 123.734\gamma - 4.596F - 188.918 \quad (13)$$

that relate to Eq. 10.  $\text{H}_2\text{O}$  contents for the 11 grains, estimated by averaging the results from Equations 12 and 13, appear reasonable (Table 4). The value thus obtained for the White Well cordierite, namely 1.69 weight percent, is identical to the value obtained by chemical analysis (Pryce, 1973). The post-heating  $\text{H}_2\text{O}$  contents estimated for Be-rich cordierites #6 and 9 indicate that they retained significant  $\text{H}_2\text{O}$  after heating at  $800^\circ\text{C}$  for six hours. Recent work (Armbruster and Bloss, in preparation) indicates that  $\text{H}_2\text{O}$  contents estimated from Eqs. 10 to 13 will be too high to the extent that  $\text{CO}_2$  also occupies the channels. In such case the "estimated  $\text{H}_2\text{O}$  content" will include  $\text{CO}_2$  content as well.

#### Variations in $2V_x$

$2V_x$  plots erratically relative to  $F$  for unheated cordierites (Fig. 2A) but less so after heating (Fig. 2B). Heating increased  $2V_x$  for the optically (-) grains but decreased it for (+) grains. Multiple linear regressions were performed using  $2V_x$  for 666 nm as the dependent variable and with  $x$ , estimated weight percent  $\text{H}_2\text{O}$ , and the closely related variables  $F$  and  $R_a$ ,

as independent ones. Results for the 10 heated grains indicated the best two-variable model ( $R^2 = 0.957$ ) to be

$$2V_x = 90.1 - 57.8x - 4.9F$$

With data for the 11 grains prior to heating added, the best two-variable model ( $R^2 = 0.873$ ) became

$$2V_x = 91.5 - 66.0x - 7.3 \text{H}_2\text{O} \quad (14)$$

The best three-variable model, which included  $R_a$ , increased  $R^2$  by only 0.0006. The  $F$  statistics generated by the regression analysis indicated, beyond reasonable doubt, a strong negative correlation between  $2V_x$  and both Na and  $\text{H}_2\text{O}$ . Folinsbee's (1941) contention, that  $2V_x$  decreases with alkali content in cordierites, is thus verified. Later authors in 'disproving' it were misled by the similar effect of  $\text{H}_2\text{O}$ .

#### Lattice parameters

The cell edges prior to heating (Table 3) were tested statistically for any relationships to  $R_a$ ,  $x$ , and the estimated  $\text{H}_2\text{O}$  content. A multiple linear regression with cell edge  $a$  as the dependent variable and  $R_a$ ,  $x$ , and estimated  $\text{H}_2\text{O}$  as the independent variables disclosed the best single-variable model ( $r^2 = 0.678$ ) to be

$$a = 15.167 + 2.6275R_a$$

and the best two-variable model ( $R^2 = 0.994$ ) to be

$$a = 14.457 + 3.6246R_a - 0.3313x \quad (15)$$

The three-variable model involving  $\text{H}_2\text{O}$  showed an increase in  $R^2$  of only 0.0005 and the  $F$  statistics indicated, beyond reasonable doubt, that  $R_a$ , and to a lesser extent  $x$ , control  $a$ . Thus Na content causes a significant decrease in  $a$  whereas  $R_a$  causes an increase.

For cell edge  $b$ , a similar regression analysis showed  $R_a$  to be the dominant control over  $b$  with the best single-variable model ( $r^2 = 0.959$ ) being

$$b = 8.321 + 1.9324R_a$$

The best two-variable model ( $R^2 = 0.9903$ )

$$b = 8.402 + 1.803R_a + 0.0105 \text{H}_2\text{O} \quad (16)$$

was little better than the next-best two-variable model ( $R^2 = 0.9898$ )

$$b = 8.459 + 1.739 R_a + 0.064x \quad (17)$$

The nearly equal success of Eq. 16 and 17 perhaps stems from a positive correlation which exists between Na content and  $\text{H}_2\text{O}$  content in cordierites.

Table 4. Estimated water contents in weight percent for cordierite grains before heating (upper line) and after heating (lower line)

Grains	Equations Used				
	12	13	Av.	10	11
#1	1.66 0.09	1.71 -0.04	1.69 0.03	1.71 0.03	1.65
#2	0.93 0.14	1.10 0.12	1.02 0.13	1.03 0.14	0.89
#3	0.80	0.77	0.79	0.79	
#4	1.63 0.07	1.61 0.08	1.62 0.08	1.63 0.08	1.54
#5	0.91 0.11	1.11 0.10	1.01 0.11	1.03 0.10	0.91
#6	2.80 0.48	2.60 0.44	2.70 0.46	2.71 0.46	2.22
#7	1.16 0.14	1.28 0.15	1.22 0.15	1.23 0.14	1.07
#8	1.04 0.12	1.27 0.21	1.16 0.17	1.16 0.16	0.98
#9	2.60 1.18	2.59 0.55	2.60 0.87	2.59 0.83	1.74
#10	0.99 0.07	1.21 0.28	1.10 0.18	1.10 0.17	0.92
#11	1.85 0.09	1.97 0.30	1.91 0.20	1.91 0.18	1.71

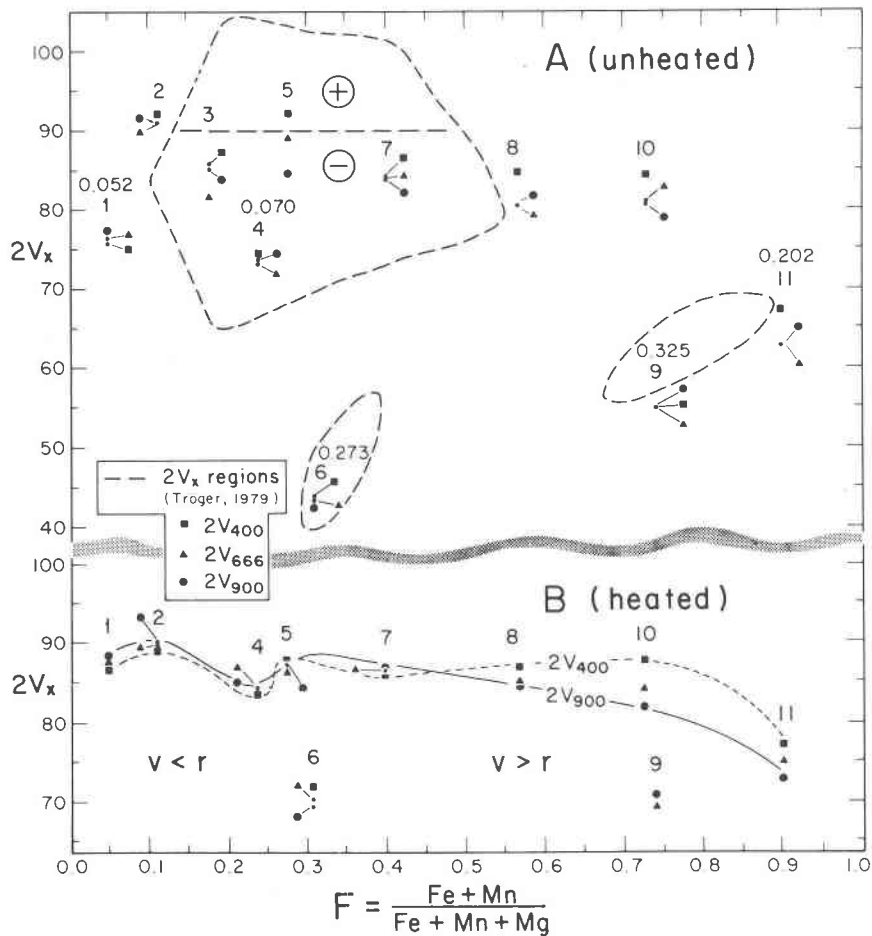


Fig. 2. Variations in  $2V_x$  vs.  $F$  for grains #1 to #11 before heating (A) and after heating (B).

If the linear regression analysis for  $a$  and  $b$  is performed on the data set for only the unheated low-Na cordierites—omitting the data of #6, #9 and #11—the best single-variable models are ( $r^2 = 0.989$ )

$$a = 14.270 + 3.862R_a \quad (18)$$

(0.006) (0.125) (0.169)

and ( $r^2 = 0.986$ )

$$b = 8.566 + 1.597R_a \quad (19)$$

(0.003) (0.058) (0.078)

The lines representing Eq. 18 and 19 are drawn in Figure 3 along with the observed data for the  $a$  and  $b$  cell edges.

A plot of cell edge  $c$  vs.  $R_a$  departs from linearity (Fig. 3). Consequently, a third-degree polynomial  $c = -221.70 + 940.43R_a - 1274.2R_a^2 + 574.64R_a^3$  (20) best fit the data ( $R^2 = 0.982$ ). A multiple linear regression analysis for  $c$ —using  $R_a$ ,  $x$ , and  $H_2O$  as inde-

pendent variables but excluding the data for specimens #9 and #11—indicated that  $R_a$  is the dominant control over  $c$ . The best single-variable model ( $r^2 = 0.982$ ) was

$$c = 10.19 - 1.168 R_a$$

whereas the best two-variable model ( $R^2 = 0.982$ ) was

$$c = 10.18 - 1.163 R_a + 0.0011 H_2O$$

The effect of  $H_2O$  on  $c$  thus seems small-to-negligible and the effect of Na seems even less. Also,  $c$  for the Haddam cordierite (#6) falls relatively “on line” in Figure 3 despite the high Na content. The upturn in the curve for  $c$ , required by the data for specimens 9, 10, and 11, cannot be attributed to the higher Mn contents of 9 and 11 because specimen 11, though it contains half as much Mn as 9, has a higher value for  $c$ , and specimen 10, moreover, lacks detectable Mn.

In several respects, the changes in cell edges  $a$ ,  $b$ ,

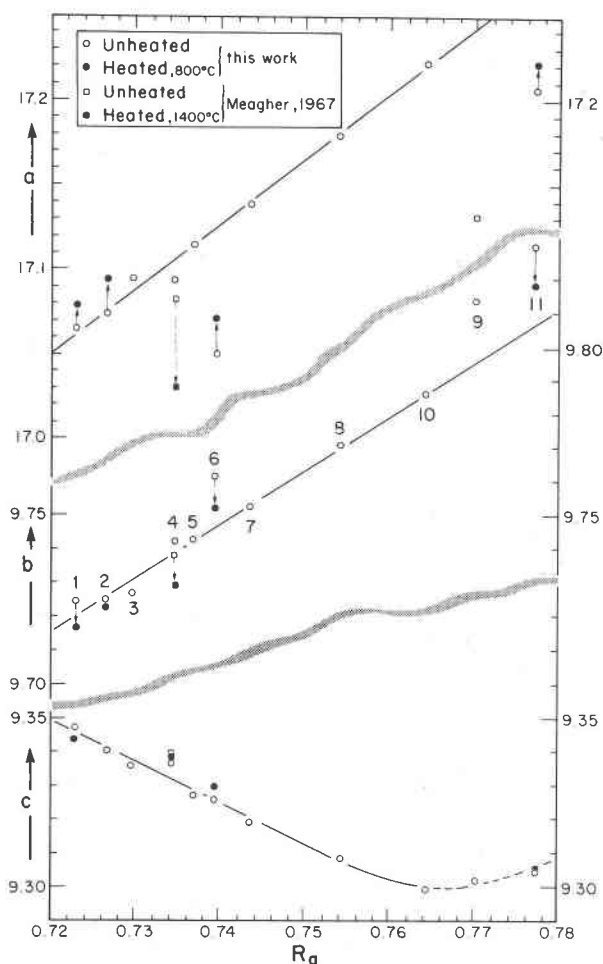


Fig. 3. Variation of cell edges  $a$ ,  $b$ , and  $c$  relative to  $R_a$ , the average radius of the ions in the octahedral sites, for grains #1 to #11 before heating (open circles) and after heating at 800°C (filled circles). For a different crystal of #4, the Guilford cordierite, Meagher's (1967) values are plotted before heating (hollow square) and after heating at 1400°C (filled square), this heating having decreased  $\Delta$  for the crystal. Note the opposite changes in cell edge  $a$  as caused by dehydration (heating at 800°C) and disordering (heating at 1400°C).

and  $c$  observed as  $R_a$  increases (Fig. 3) mimic those when Mg-cordierites are heated and, as observed by Hochella *et al.* (1979), the octahedral dimensions increase. In other words, as the octahedral volume increases, whether in response to temperature or substitution of larger  $\text{Fe}^{2+}$  or  $\text{Mn}^{2+}$  ions for  $\text{Mg}^{2+}$ , the  $a$  and  $b$  cell edges increase but  $c$  decreases. Whether the upturn in  $c$ , when  $R_a$  exceeds 0.765, correlates with increased octahedral volume is not established. Hochella *et al.* observed no upturn in  $c$  for temperatures to 775°C. In contrast, a concave-upward plot of  $c$  vs. temperatures up to 800°C was observed by Fischer *et al.* (1974) for a hexagonal cordierite and

by Morosin (1972) for the isostructural mineral beryl. Moreover, Brown *et al.* (1979) observed  $c$  for an alkali-rich beryl to increase, rather than decrease, from 24° to 800°C.

#### The distortion index $\Delta$

Values of  $\Delta$  calculated from each crystal's cell edges (Table 3) were plotted against  $R_a$  (Fig. 4). For the unheated low Na cordierites ( $x < 0.08$ ) the points fall along a line, whereas those for the three high-Na specimens fall much below this line. Quite clearly,  $\Delta$  decreases markedly as Na content increases, largely because the  $a$  cell edge decreases so markedly with Na content (whereas the  $b$  and  $c$  cell edges seem little affected).

A multiple linear regression using  $\Delta$  as the dependent variable and  $R_a$ ,  $x$ , and estimated  $\text{H}_2\text{O}$  content as the independent variables indicated that, for the 11 cordierites prior to heating, the best single-variable model for predicting  $\Delta$  involved Na, namely ( $r^2 = 0.952$ )

$$\Delta = 0.282 - 0.435x$$

The best two-variable model ( $R^2 = 0.985$ ),

$$\Delta = -0.143 - 0.480x + 0.577R_a \quad (21)$$

(0.007)   (0.099)   (0.022)   (0.135)

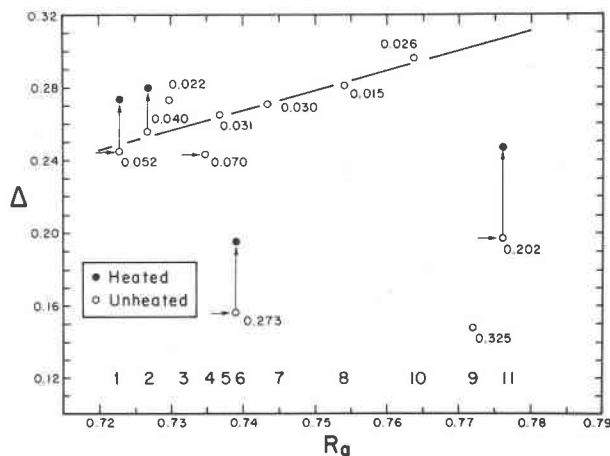


Fig. 4. Distortion index vs.  $R_a$  for the grains prior to heating (open circles) and for the four measured after heating (filled circles). The value for  $x$ , the Na atoms per formula unit, is also added. Horizontal arrows designate data points for crystals from the same specimen as were crystals for which previous investigators demonstrated perfect or near-perfect Al/Si ordering by neutron or X-ray diffraction. The line shown is that derived from a least-squares linear regression analysis of the data for the low-Na cordierites ( $x < 0.08$ ). Consequently, values of  $\Delta$  calculated using cell edges taken from the regression lines in Fig. 3 also plot on this line. The high-Na cordierites ( $x > 0.08$ ) plot below this line roughly in proportion to their value for  $x$ .

included  $R_a$ . The three-variable model, which included  $H_2O$ , was not significantly better ( $R^2 = 0.986$ ) than Eq. 21. The  $F$  statistics also indicated  $\Delta$  to be controlled dominantly by  $x$ , less so by  $R_a$ , but not by water. This seemed puzzling because, when four cordierites were heated to drive off  $H_2O$  (but not Na),  $\Delta$  increased significantly. This over-shadowing by Na of the effect of  $H_2O$  on  $\Delta$  we attribute to the high correlation between Na and  $H_2O$  content in unheated cordierites—for example, linear regression yielded the model ( $r^2 = 0.875$ )

$$H_2O = 0.99 + 5.389x \quad (22)$$

During the regression analysis that yielded Eq. 21, the  $x$  term apparently accommodated for the effect on  $\Delta$  not only of  $Na^+$  but also of  $H_2O$ .

With the data for the four heated cordierites also included in the regression analysis, the best three-variable model for predicting  $\Delta$  ( $R^2 = 0.985$ ) was

$$\Delta = 0.500R_a - 0.363x - 0.020 H_2O - 0.067 \quad (23)$$

The  $F$  statistics now indicated that  $H_2O$  had a significant effect on  $\Delta$ , less than Na but now more than  $R_a$ . Possibly, if 'after-heating' values for  $\Delta$  for all 11 cordierites had been available and included in the regression analysis, the effect of  $H_2O$  on  $\Delta$  may even have proved more significant than that of Na.

Stout's (1975) observation that  $H_2O$  content affects  $\Delta$  is thus substantiated. In further confirmation, Schreyer (1979) observed  $\Delta$  to change from  $0.12^\circ$  to  $0.26^\circ$  when a Na,Be cordierite from Soto, Argentina was dehydrated by heating in air at  $1000^\circ C$  for two hours. Following rehydration of the specimen at  $P_{H_2O}$  of 2 kbar at  $700^\circ C$  for 24 hours,  $\Delta$  returned to  $0.11^\circ$ .

Crystals 1, 4, 6, and 11 most likely possess perfect or near-perfect Al/Si ordering. We conclude this because they derive from the same specimens as did crystals for which crystal-structure analyses (Gibbs, 1966; Meagher, 1967; Cohen *et al.*, 1977; Hochella *et al.*, 1979) disclosed such ordering. Moreover, their  $\Delta$  values compare closely to those for these structurally analyzed crystals. Thus  $\Delta$  equals  $0.245^\circ$  for our crystal #1 whereas for White Well crystals structurally analyzed by Cohen *et al.* it was  $0.24^\circ$  (neutron diffraction) and  $0.25^\circ$  (X-ray diffraction), and for that structurally analyzed by Hochella *et al.* it was  $0.25^\circ$ . Although Al/Si ordering for crystal #1 thus seems assured, it plots at the lower end of the regression line for low-Na cordierites (Fig. 4). Consequently, *the upward slope of this line cannot be attributed to an increase in already perfect Al/Si ordering but to a compositional effect, namely, increase in  $R_a$ .* Furthermore,

perfect or near-perfect Al/Si ordering may also be presumed for crystals 4, 6, and 11, yet  $\Delta$  for them plots below the low-Na cordierites' regression line, roughly in proportion to Na content.

Eq. 23 predicts  $\Delta$  to within 0.003 for the four heated cordierites and, except for specimens 10 and 11, to within 0.007 for the 11 cordierites prior to heating. Eq. 21 is almost equally successful for the 11 unheated cordierites but errs by as much as 0.05 for the heated (dehydrated) cordierites. The success of Eq. 23, though it lacks a term for Al/Si ordering, further enforces the emerging conclusion that Al/Si ordering has little or no significant effect on  $\Delta$  for the cordierites we studied. Eq. 23 predicts  $\Delta$  to be 0.149 for specimen 9 whereas measured  $\Delta$  was 0.148. This, the lowest  $\Delta$  value here observed, is thus explained entirely by compositional effects.

The results of Graziani and Guidi's (1978) study of a cordierite from Madagascar indicate:  $R_a$ , 0.722;  $x$ , 0.033;  $F$ , 0.058;  $\alpha$ , 1.528;  $\beta$ , 1.532;  $\gamma$ , 1.537;  $\beta$  (after dehydration at  $1400^\circ C$ ), 1.522;  $\Delta$ , 0.26;  $H_2O$ , 2.5 weight percent. These optical constants and the  $H_2O$  content merit verification because Eq. 10—using their values for  $F$ ,  $\alpha$ , and  $\gamma$ —estimates  $H_2O$  at only 0.87 weight percent. Moreover, if we accept the difference in  $2\beta$  before and after heating as approximately the value of  $(\alpha + \gamma)$  before and after heating, then inserting this value (0.020) into Eq. 11 yields an  $H_2O$  content of 1.31 weight percent. Eq. 21, which lacks a term for  $H_2O$ , calculates  $\Delta$  to be  $0.26^\circ$ , precisely the value they observed. However, Eq. 23, which includes a term for  $H_2O$ , predicts  $\Delta$  to be  $0.232^\circ$  (if  $H_2O$  equals 2.5 weight percent),  $0.256^\circ$  (if  $H_2O$  equals 1.31), and  $0.265^\circ$  (if  $H_2O$  equals 0.87). For  $H_2O$  equal to zero, Eq. 23 predicts  $\Delta$  to be  $0.282^\circ$ , which compares to the value 0.29 Graziani and Guidi obtained after heating the crystal to  $800^\circ$ ,  $900^\circ$ ,  $1000^\circ$ , or  $1100^\circ C$ . For this natural cordierite, therefore,  $\Delta$  also appears independent of Al/Si ordering.

### Conclusions

(1) Heated at  $800^\circ C$  for six hours in  $H_2$  atmosphere, cordierites lose  $H_2O$  but not Na. However, crystals with high Na and Be contents resist complete dehydration so that, even after heating, their refractive indices plot above the otherwise highly regular trends for heated cordierites. This may permit easy recognition of Be-rich cordierites or of those with very high Na contents.

(2) Orthorhombic cordierites have low  $2V$  values in proportion to their  $H_2O$  content and, since high Na content correlates with high  $H_2O$  content, in pro-

portion to their Na content. Dehydration increases  $2V_x$  except for (+) cordierites. When  $2V_x$  is less than  $70^\circ$  for unheated crystals, significant  $\text{Na}^+$  and  $\text{H}_2\text{O}$  are likely present.

(3) As  $R_a$ , the average radius of the ion in the octahedral site, increases, the  $a$  and  $b$  cell edges increase markedly whereas  $c$  at first decreases, attains a poorly defined minimum, and then increases.

(4) With Na content, cell edge  $a$  decreases significantly,  $b$  (if anything) increases, and thus  $\Delta$  decreases. Octahedral vacancies, which microprobe analyses reveal to correlate with Na content, may contribute, perhaps entirely, to these cell edge variations. Wallace and Wenk (1980) observe significant vacancies on the octahedral and tetrahedral sites in cordierite and suspect that they correlate with the presence of cations in the channels.

(5) For the 11 cordierites here studied,  $\Delta$  correlates entirely with compositional factors (cf. Eq. 23). For 4 of the 11 specimens, crystal structure analyses (on other crystals) have indicated perfect or near-perfect Al/Si ordering and, for reasons discussed, all 11 likely possess such ordering. If natural orthorhombic cordierites truly represent a spectrum of structural states, the 11 ordered cordierites studied here represent a remarkably biased sample which must be further enlarged by addition of the hydrous cordierite from Madagascar described by Graziani and Guidi (1978)—and by any other cordierite for which Eq. 23 successfully predicts  $\Delta$  from composition alone.

(6) Crystal structure analysis of cordierites to determine Al/Si ordering should be narrowed down to cordierites for which Eq. 23 fails to predict  $\Delta$ . If perfect Al/Si ordering is demonstrated for such cordierites, a compositional control of  $\Delta$  outside those embraced in Eq. 23 may be discovered.

(7) On the basis of present evidence, it appears that all natural orthorhombic cordierites will likely have perfect or near-perfect Al/Si ordering and that disordering is confined to the indialites, whose conditions of formation and cooling differ markedly from metamorphic or pegmatitic cordierites.

### Acknowledgments

We are grateful to Professor G. V. Gibbs, who read the manuscript and freely contributed specimens and advice. We thank Professor Paul Ribbe, who maintained a lively interest in the study and determined beryllium for the Dolni Bory specimen (by ion-probe). He and Todd Solberg aided and advised the writers so that the microprobe analyses of the 11 grains would be of high quality. Discussions and ideas contributed by Thomas Armbruster are also appreciated. Important cordierite specimens were kindly provided

by John S. White of the Smithsonian Institute and by J. Alexander Speer. We thank Professor H. R. Wenk (University of California) for supplying a preprint of the Wallace and Wenk paper.

### References

- Barr, A. J., J. H. Goodnight, J. P. Sall and J. T. Helwig (1976) *A User's Guide to SAS*. SAS Institute Inc., P. O. Box 10066, Raleigh, North Carolina 27605.
- Bloss, F. D. (1978) The spindle stage: a turning point for optical crystallography. *Am. Mineral.*, 63, 433–447.
- (in press) *The Spindle Stage: Principles and Practice*. Cambridge University Press, Cambridge and New York.
- and D. Riess (1973) Computer determination of  $2V$  and indicatrix orientation from extinction data. *Am. Mineral.*, 58, 1052–1061.
- Brown, G. E., Jr., M. F. Hochella, Jr. and B. A. Mills (1979) The effects of temperature on beryl–cordierite-type framework silicates (abstr.). *Am. Crystallographic Assoc., Program and Abstracts, Series 2*, 6, No. 2.
- Burnham, C. W. (1962) Lattice constant refinement. *Carnegie Inst. Wash. Year Book*, 61, 132–135.
- (1965) Refinement of lattice parameters using systematic correction terms. *Carnegie Inst. Wash. Year Book*, 64, 200–202.
- Černý, P. and F. C. Hawthorne (1976) Refractive indices versus alkali contents in beryl: general limitations and applications to some pegmatitic types. *Can. Mineral.*, 14, 491–497.
- Cohen, J. P., F. K. Ross and G. V. Gibbs (1977) An X-ray and neutron diffraction study of hydrous low-cordierite. *Am. Mineral.*, 62, 67–78.
- Fischer, G. R., D. L. Evans and J. E. Geiger (1974) Crystal lattice thermal expansion of cordierite (abstr.). *Am. Crystallographic Assoc., Program and Abstracts, Series 2*, 2, 214.
- Folinsbee, R. E. (1941) Optic properties of cordierite in relation to alkalis in the cordierite–beryl structure. *Am. Mineral.*, 26, 485–500.
- Gibbs, G. V. (1966) The polymorphism of cordierite I: the crystal structure of low cordierite. *Am. Mineral.*, 51, 1068–1087.
- Goldman, D. S., G. R. Rossman and W. A. Dollase (1977) Channel constituents in cordierite. *Am. Mineral.*, 62, 1144–1157.
- Graziani, G. and G. Guidi (1978) Hydrous gem magnesian cordierite with inclusions of hydroxyapatite, dolomite, and rutile. *Mineral. Mag.*, 42, 481–485.
- Harwood, D. S. and R. R. Larson (1969) Variations in the delta index of cordierite around the Cupsuptic pluton, west-central Maine. *Am. Mineral.*, 54, 896–908.
- Hawthorne, F. C. and P. Černý (1977) The alkali-metal positions in Cs–Li beryl. *Can. Mineral.*, 15, 414–421.
- Hochella, M. F., Jr., G. E. Brown, Jr., F. K. Ross and G. V. Gibbs (1979) High-temperature crystal chemistry of hydrous Mg- and Fe-rich cordierites. *Am. Mineral.*, 64, 337–351.
- Iiyama, T. (1956) Optical properties and unit cell dimensions of cordierite and indialite. *Mineral. J.*, 1, 372–394.
- Kaminen, D. C. (1974) Variation in the distortion index of cordierite east of the Sparrow Lake granite pluton, District of Mackenzie. *Can. Mineral.*, 12, 419–421.
- Langer, K. and W. Schreyer (1976) Apparent effects of molecular water on the lattice geometry of cordierite: a discussion. *Am. Mineral.*, 61, 1036–1040.
- Leake, B. E. (1960) Compilation of chemical analysis and physical constants of natural cordierites. *Am. Mineral.*, 45, 282–298.
- Lepezin, G. G., I. K. Kuznetsova, Yu. G. Lavrent'ev and O. S.

- Chmel'nicova (1976) Optical methods of determination of the water contents in cordierites. *Contrib. Mineral. Petrol.*, 58, 319–329.
- Louisnathan, S. J., F. D. Bloss and E. J. Korda (1978) Measurement of refractive indices and their dispersion. *Am. Mineral.*, 63, 394–400.
- Meagher, E. P. (1967) *The Crystal Structure and Polymorphism of Cordierite*. Ph.D. Dissertation, The Pennsylvania State University, University Park, Pennsylvania.
- Medenbach, O., W. V. Maresch, P. W. Mirwald and W. Schreyer (1979) Optische Bestimmung des H<sub>2</sub>O-Gehalts synthetischer Mg-Cordierite. *Fortschritte der Mineralogie*, 57, Beiheft 1, 99–101.
- Miyashiro, A. (1957) Cordierite–indialite relations. *Am. J. Sci.*, 255, 43–62.
- Morosin, B. (1972) Structure and thermal expansion of beryl. *Acta Crystallogr.*, B28, 1889–1893.
- Newton, R. C. (1966) BeO in pegmatitic cordierite. *Mineral. Mag.*, 35, 920–927.
- Povondra, P. and K. Langer (1971) Synthesis and some properties of sodium–beryllium-bearing cordierite, Na<sub>x</sub>Mg<sub>2</sub>(Al<sub>4-x</sub>Be<sub>x</sub>Si<sub>5</sub>O<sub>18</sub>). *Neues Jahrb. Mineral. Abh.*, 116, 1–19.
- Pryce, M. W. (1973) Low-iron cordierite in phlogopite schist from White Well, Western Australia. *Mineral. Mag.*, 39, 241–243.
- Robertson, D. K. and R. E. Folinsbee (1974) Lead isotope ratios and crustal evolution of the Slave Craton at Ghost Lake, Northwest Territories. *Can. J. Earth Sci.*, 11, 819–827.
- Schreyer, W. (1959) Natural cordierite-bearing rocks. *Carnegie Inst. Wash. Year Book*, 58, 96–98.
- (1979) Natrium–Beryllium Cordierite und ihre ungewöhnlichen Eigenschaften bei Veränderung des Wassergehaltes. *Fortschritte der Mineralogie*, 57, Beiheft 1, 143–144.
- and H. S. Yoder, Jr. (1964) The system Mg-cordierite–H<sub>2</sub>O and related rocks. *Neues Jahrb. Mineral. Abh.*, 101, 271–342.
- Shannon, R. D. (1976) Revised effective ionic radii and systematic studies of interatomic distances in halides and chalcogenides. *Acta Crystallogr.*, A32, 751–767.
- Speer, J. A. (1976) *The Stratigraphy and Metamorphism of the Snyder Group, Labrador*. Ph.D. Thesis, Virginia Polytechnic Institute and State University, Blacksburg, Virginia.
- Stanek, J. and J. Miskovsky (1964) Iron-rich cordierite from a pegmatite near Dolni Bory, W. Moravia, Czechoslovakia. *Časopis pro Mineralogii a Geologii*, 9, 191–192.
- Stout, J. H. (1975) Apparent effects of molecular water on the lattice geometry of cordierite. *Am. Mineral.*, 60, 229–234.
- Tröger, W. E. (1979) *Optical Determination of Rock-forming Minerals*, 4th Ed. by H. U. Bambauer, F. Taborszky and H. D. Trochim. E. Schweizerbart'sche Verlagsbuchhandlung, Stuttgart, Germany.
- Wallace, J. H. and H. R. Wenk (1980) Structure variation in low cordierites. *Am. Mineral.*, 65, 96–111.

Manuscript received, May 15, 1979;  
accepted for publication, December 11, 1979.